TURBULENT FLOW ACROSS A ROTATING CYLINDER WITH SURFACE ROUGHNESS

Everts, M., Ebrahim R., Kruger, J.P., Miles, E., Sharifpur M.* and Meyer, J.P.
*Author for correspondence
Department of Mechanical and Aeronautical Engineering,
University of Pretoria,
Pretoria, 0002,
South Africa,
E-mail: mohsen.sharifpur@up.ac.za

ABSTRACT

The purpose of this study was to investigate the influence of surface roughness on turbulent flow across a rotating cylinder. Although smooth rotating cylinders have been extensively investigated, the influence of surface roughness on flow across rotating cylinders has not been reported yet. The parameters for the analysis were chosen such that the Reynolds number is sufficiently large in order to avoid vortex shedding behind the cylinder, while still sufficiently low to maintain the assumption of incompressible flow. Three different Reynolds numbers (5×10^5, 10^6 and 5×10^6) and rotation rates ($\alpha = 1$, 2 and 3) were investigated using four different surface roughnesses ($\varepsilon/D = 0$, 0.0011, 0.0045 and 0.009) and a validated CFD model. The drag coefficients decreased with increasing Reynolds number due to the turbulent boundary layer that moves the separation bubble further to the rear of the body. Increasing surface roughness increased the drag coefficient, but this increase became less as the Reynolds number increased. The lift coefficient increased with increasing Reynolds number, surface roughness and rotation rate. The investigated Reynolds number range is very desirable since the drag decreased while the lift increased. Furthermore, the aerodynamic efficiency revealed that the most aerodynamic efficient case occurs at a combination of the largest surface roughness, Reynolds number and rotation rate.

INTRODUCTION

It was first shown by Magnus in 1953 that rotation causes the occurrence of a lift force [1]. Since then, a lot of effort has been made to use the benefits of this effect in practical applications and to understand this effect better. Therefore, extensive theoretical, numerical and experimental investigations have been done on flow over rotating cylinders. Its engineering applications include heat transfer from rotating machinery, design of rotating heat exchangers, rotating cylinder wings, spinning projectiles, drying of paper, and it can even be used instead of sails to propel ships. Rotation can be used to delay or suppress vortex shedding and therefore to extend the steady flow regime. Furthermore, it can also be used for flow control, lift enhancement, boundary layer control, etc. Although a cylinder is the simplest bluff body shape and is free from geometrical singularities, it provides excellent insights into the physics of flow, for example the wake phenomena, vortex shedding, and drag and lift characteristics.

Investigations of flow past a rotating cylinder have been conducted by several researchers; however, these investigations were mainly limited to laminar flow [1-12]. High Reynolds number flows over cylinders are complicated due to the coupled action of the shear layer instability and the early development of the fully turbulent attached boundary layer, as well as the more pronounced three dimensional effects. High Reynolds number flows have been mainly investigated for non-rotating cylinders, and up to now, only a few investigations of turbulent flow across rotating cylinders have been conducted [13-15].

NOMENCLATURE

C	[-]	Coefficient
D	[m]	Diameter of cylinder
F	[N]	Force
u_∞	[m/s]	Free stream velocity
Special characters		
α	[-]	Non-dimensional rotation rate
ε	[m]	Roughness height
ν	[m²/s]	Kinematic viscosity
ω	[rad/s]	Rotation rate
Subscripts		
d		Drag
l		Lift

The effect of surface roughness on the flow across a circular cylinder was first investigated by Fage and Warsap in 1930. Achenbach [16] found in his investigations that the critical Reynolds number is decreased when the surface roughness is increased. The critical Reynolds number is when the drag coefficient is a minimum. Furthermore, surface roughness causes a more regular transition to turbulent flow and the separation line is also straightened. The influence of surface roughness on turbulent flow across a stationary cylinder has been extensively investigated, while fewer investigations were done on laminar flow since it was found that roughness has very little effect on the drag coefficient [17].

According to the authors' best knowledge, no previous investigations were reported on the influence of surface roughness on flow across a rotating cylinder. Therefore, the aim of this study is to investigate turbulent flow across a rotating cylinder with surface roughness. Three different Reynolds numbers ($5x10^5$, 10^6 and $5x10^6$) will be investigated using different surface roughnesses ($\varepsilon/D = 0$, 0.0011, 0.0045 and 0.009) and rotation rates ($\alpha = 1$, 2 and 3).

NUMERICAL MODELLING
Governing Equations and Turbulence Modelling
The built-in governing equations and turbulent constants of ANSYS FLUENT were used.

The rotational rate is defined as:

$$\alpha = \frac{\frac{1}{2}\omega D}{V} \qquad (1)$$

The integral forms for the force coefficients are as [18]:

$$c_n = \frac{1}{c}\left[\int_0^c (C_{p,l} - C_{p,u})dx + \int_0^c \left(C_{f,u}\frac{dy_u}{dx} + C_{f,l}\frac{dy_l}{dx}\right)dx\right] \qquad (2)$$

$$c_a = \frac{1}{c}\left[\int_0^c \left(C_{p,u}\frac{dy_u}{dx} - C_{p,l}\frac{dy_l}{dx}\right)dx + \int_0^c (C_{f,u} + C_{f,l})dx\right] \qquad (3)$$

The lift and drag coefficients are defined as following [18]:

$$c_l = c_n \cos\alpha - c_a \sin\alpha \qquad (4)$$

$$c_d = c_n \sin\alpha + c_a \cos\alpha \qquad (5)$$

Although there are several commonly-used computational models that are used for turbulent flows, the Reynolds-averaged Navier-Stokes (RANS) and Large eddy simulation (LES) models are mostly used to model flow across cylinders. LES is significantly more computationally expensive than RANS; therefore a steady RANS model was used for this study. According to Karabelas et al. [15] there is no vortex shedding at high Reynolds numbers. To verify this, a transient analysis at a Reynolds number of $5x10^5$ and rotation rate of 1 was conducted. The results showed that a single vortex was shed

and thereafter no vortices were generated, therefore, a steady RANS model is sufficient. The k-ε turbulence model is one of the most common models used since it is robust in a variety of applications, computationally cheap, easy to implement, and has a good convergence rate. The model is a two equation model that consists of two extra transport equations. The transport variables are the turbulent kinetic energy and turbulent dissipation rate, which determine the scale of the turbulence and the energy in the turbulence, respectively. The standard k-ε turbulence model is used to predict the flow over the cylinder, since it generates results that correlate well with the experimental results obtained by Warschauer [19] in Figure 3. Although the k-ε model may be disadvantageous in modelling separated flow, it performed better than other turbulence models and showed good correlation with the experimental results of Warschauer.

Computational Grid
The flow problem is modelled as a two-dimensional circular cylinder which resides in a circular flow domain. The origin of the Cartesian coordinate system lies at the centre of the cylinder with the cylinder's axis perpendicular to the free stream (flowing left to right) as illustrated in Figure 1. The placement of the far field boundaries must be located far enough to avoid any effect on the flow near the cylinder. Mittal and Kumar [8] conducted a boundary location study and found that the force and moment coefficients remain constant for the outer boundaries located at 75 times the diameter of the cylinder. Therefore, similar to Karabelas et al. [15], a conservative distance of 100 times the diameter of the cylinder was selected for the present study.
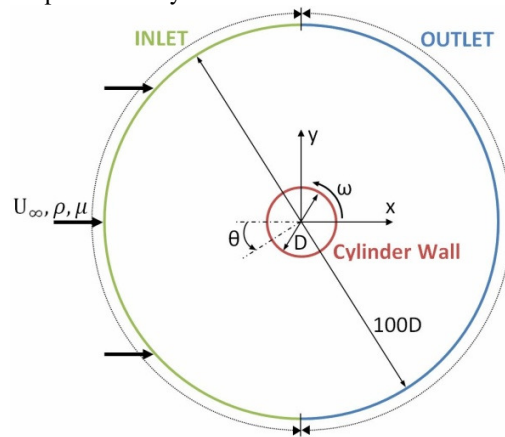

Figure 1: Computational domain with boundaries and dimensions

In order to determine the coarsest mesh that can be used to simulate the flow across a rotating cylinder, while retaining a high level of accuracy, a mesh independence study was conducted. The final grid is shown in Figure 2 and divided the flow domain into 270 circumferential divisions and 301 radial divisions resulting in 162 554 quadrilateral elements and 163 110 nodes. The mesh is clustered near the cylinder surface to capture the boundary layer.

Appropriate boundary conditions are required to solve the governing equations, therefore along the impermeable cylinder wall, a uniform roughness was specified together with a no-slip velocity boundary condition. Moreover, in order to generate relative motion between the cylinder and the fluid, a constant angular velocity was specified along the cylinder axis in a counter-clockwise direction. A uniform free stream velocity boundary condition was applied at the boundary upstream of the cylinder. At the boundary downstream of the cylinder, a pressure-outlet boundary condition was prescribed. The boundary conditions are summarised in Table 1.
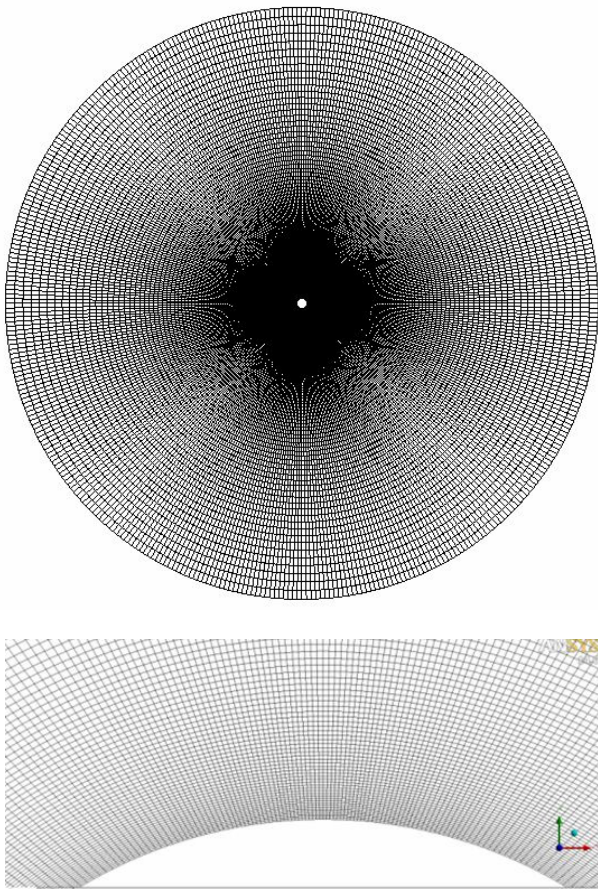

Figure 2: Mesh for numerical simulation

Table 1: Boundary Conditions

Boundary	Conditions at 288.16 K
Inlet	x-velocity: u_∞ [m/s] y-velocity: 0 [m/s]
Outlet	Gauge Pressure: 0 [Pa]
Cylinder Wall	No-slip condition Angular velocity [rad/s] Relative roughness

Numerical Simulation

In this study, a steady-state simulation was conducted to predict how an incompressible viscous fluid behaves as it passes over a rotating cylinder. The continuity and momentum equations are discretised by means of the finite volume method resulting in a system of algebraic equations. These equations are solved using FLUENT (version 14.5) and second order upwind scheme was used to discretise the convective terms in the momentum equations. The standard k-ε turbulence model with standard wall treatment was selected for the present study. In order to solve the pressure-velocity coupling equations, the semi-implicit method for pressure-linked equations (SIMPLE) algorithm was used. A convergence criteria of 10^{-8} for the residuals of the continuity and momentum equations were prescribed.

Validation

The CFD model was validated by comparing the pressure coefficients for a stationary case at Re = 1.26×10^6 with the experimental results obtained by Warschauer [19]. From Figure 3 it can be observed that the trend of both data sets is similar and there is good agreement between them. The present results deviate slightly from the results of Warschauer between θ = 80° and θ = 140°. Possible reasons for the slight deviation may be the simplifications of the CFD model and the fact that a 2D model was simulated while experimental data was used for the validation. Validating the results with experimental data proves that the numerical model agrees with the physical reality and serves as sufficient evidence that the selected turbulence model will generate accurate results for other flow scenarios.
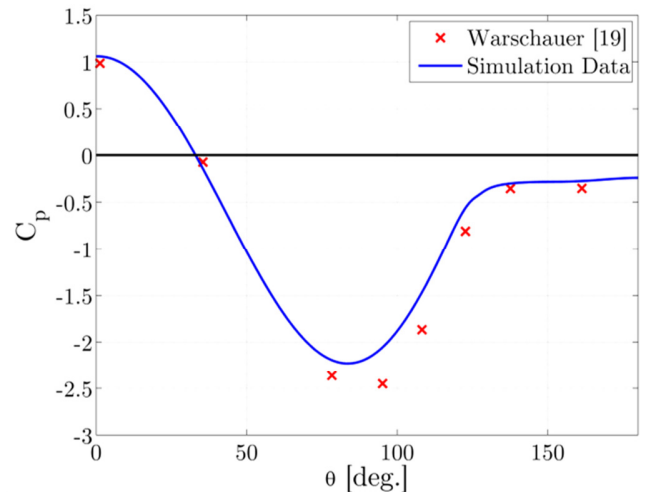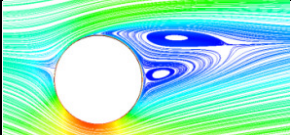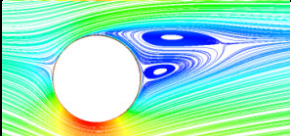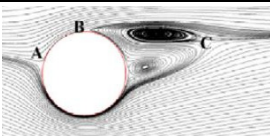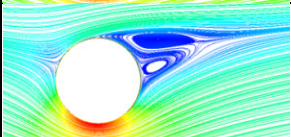

Figure 3: Validation of pressure coefficient
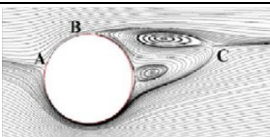
To further validate the CFD model, the streamlines for three different Reynolds numbers at a rotation rate of α = 2 were also compared with the results obtained by Karabelas et al. [15]. The results are summarised in Table 2 and it can be concluded that both stagnation points (A and B) as well as the two vortex structures were accurately captured and the CFD model is therefore validated.

Table 2: Validation of Streamlines

Re	Present Study	Karabelas et al. [15]
5×10^5		
10^6		
5×10^6		

RESULTS

The streamlines for different values of Reynolds number and surface roughness, at a rotation rate of α = 2, are shown in Figure 4. From this figure it follows that the friction between the fluid and the surface of the cylinder drags the fluid along the cylinder surface. Due to the counter-clockwise circulation, there is an "extra" velocity contribution at the bottom of the cylinder. This leads to a higher velocity at the bottom of the cylinder and a lower velocity at the top of the cylinder. Furthermore, the stagnation point at the nose of the body is independent of surface roughness since it remains at the same position for different values of surface roughness. However, the stagnation point is dependent on Reynolds number and moves slightly upward with increasing Reynolds numbers.
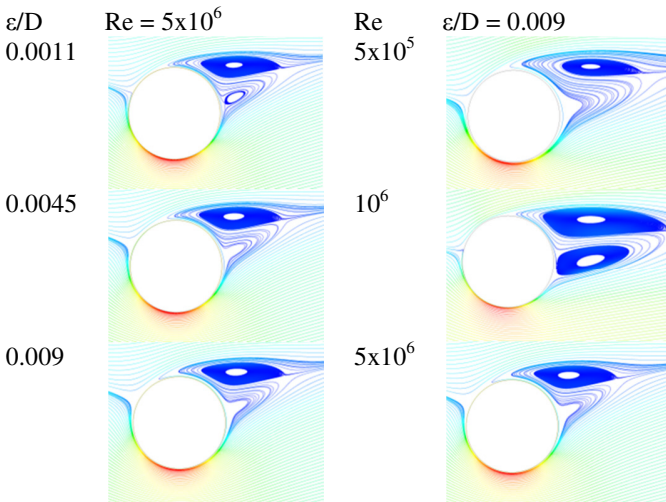

Figure 4: Streamlines for different Reynolds numbers and surface roughness at a rotation rate of α = 2

The streamline plots for a surface roughness value of ε/D = 0.009 and different rotation rates and Reynolds number range are summarised in Figure 5. Once again it can be concluded that the velocity reaches a maximum at the bottom of the cylinder. The pressure at the bottom of the cylinder is lower than on the top of the cylinder and this imbalance pressure creates a net downward force that is a finite lift. The cylinder rotated counter-clockwise in the CFD simulations. Therefore, a downward net force is created, instead of an upward force which is created when a cylinder rotates clockwise. The stagnation point at the nose of the cylinder moves slightly upward for both increasing Reynolds numbers and rotation rates. The separation point is also dependent on Reynolds number and moves counter-clockwise with increasing Reynolds. Furthermore, the size of the separation bubble increases with increasing Reynolds number but decreases with increasing rotation rate.

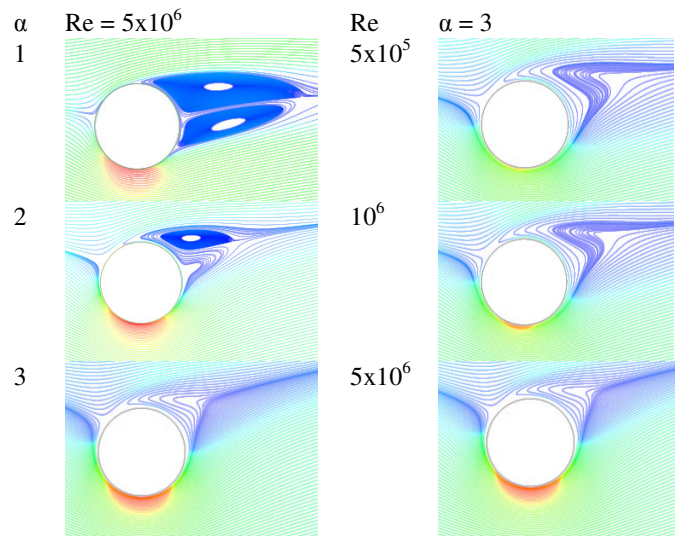**Figure 5:** Streamlines for different Reynolds numbers and rotation rates at ε/D = 0.009

In Figure 6 the rotation rate was kept constant at α = 2 while the surface roughness and Reynolds number were varied in order to investigate the influence of surface roughness and Reynolds number.
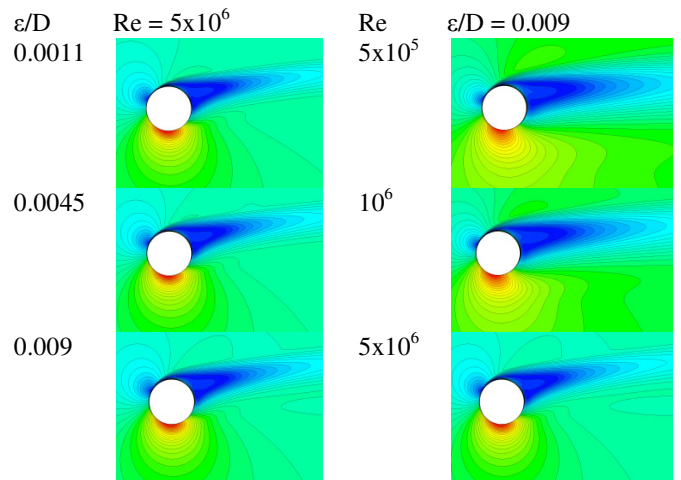

Figure 6: Velocity contours for different Reynolds number and surface roughness at a rotation rate of α = 2

In Figure 7 the effect of rotation rate and Reynolds number were investigated at a fixed surface roughness of $\varepsilon/D = 0$.
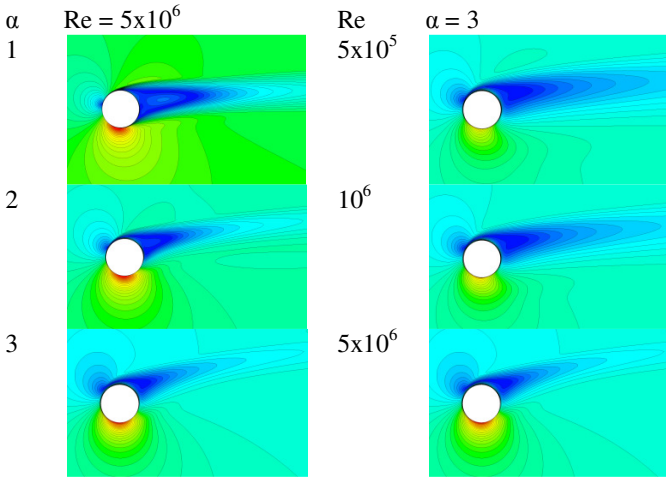

Figure 7: Velocity contours for different Reynolds numbers and rotation rates

The filled velocity contour plots are another way to investigate the separation regions. The separation regions are located at the position which the velocity is very low or zero, therefore, they are the dark blue regions. From Figures 6 and 7 it follows that the size of the separation bubble decreases with both increasing Reynolds number and surface roughness.

It has been proven theoretically that the drag on a cylinder in an inviscid, incompressible flow is zero, regardless of whether or not the flow has circulation about the cylinder. Viscous effects cause skin friction and flow separation which always produce a finite drag in real life. The drag coefficients for different combinations of Reynolds number, surface roughness and rotation rate are summarised in Tables 3 and 4.

Table 3: Drag and lift coefficients for different Reynolds and surface roughness at a rotational rate of $\alpha = 3$

ε/D	C_d	C_l
Re = 5×10^5		
0.0000	0.59948	-2.64882
0.0011	0.62122	-3.10843
0.0045	0.62849	-3.45649
0.0090	0.63304	-3.66630
Re = 10^6		
0.0000	0.47842	-3.01373
0.0011	0.48850	-3.59904
0.0045	0.48731	-3.99727
0.0090	0.48698	-4.23809
Re = 5×10^6		
0.0000	0.21802	-4.82202
0.0011	0.20740	-5.93046
0.0045	0.19849	-6.56398
0.0090	0.19362	-6.92267

From Table 3 it follows that the drag coefficient of the smooth cylinder decreases with increasing Reynolds number. This phenomenon holds for each case where the surface roughness is kept constant and the Reynolds number is increased. The large reduction in drag coefficient with increasing Reynolds number is due to the flow in the boundary layer becoming turbulent, which moves the separation bubble further to the rear of the body.

Table 4: Drag and lift coefficients for different rotation rates and surface roughness at a Reynolds number of 5×10^6

ε/D	C_d	C_l
$\alpha = 1$		
0.0000	0.205866	-2.62921
0.0011	0.322988	-2.0727
0.0045	0.352679	-2.11177
0.0090	0.356008	-2.24523
$\alpha = 2$		
0.0000	0.21470	-4.00553
0.0011	0.23918	-4.43819
0.0045	0.24724	-4.64094
0.0090	0.25155	-4.76268
$\alpha = 3$		
0.0000	0.21802	-4.82202
0.0011	0.20740	-5.93046
0.0045	0.19849	-6.56398
0.0090	0.19362	-6.92267

It can be concluded from Table 4 that the lift coefficient is strongly dependent on the rotation rate, especially at low angular velocities. In a certain Reynolds number range, as the range used in this study, the Reynolds number produces the desirable effect of increasing the lift coefficient while decreasing the drag coefficient, like with golf balls. The large reduction in drag coefficient with increasing Reynolds number is due to the flow boundary layer becoming turbulent, which moves the separation bubble further on the rear of the body. The aerodynamic efficiency is defined as the ratio of the lift coefficient to the drag coefficient:

$$\text{Aerodynamic efficiency} = \frac{C_L}{C_D} \qquad (12)$$

The aerodynamic efficiencies for the different Reynolds number and surface roughness cases are tabulated in Table 5. The lift coefficient values were multiplied by negative one to account for the counter-clockwise rotation. From this table it can be concluded that the most aerodynamic efficient case occurs at a combination of the largest surface roughness, Reynolds number and rotation rate.

Table 5: Aerodynamic efficiency for the various cases

	$\alpha = 1$	$\alpha = 2$	$\alpha = 3$
ε/D		Re = 5×10^5	
0.0000	3.148821	3.901834	4.418526
0.0011	3.062421	4.042919	5.003742
0.0045	2.965087	4.220853	5.499635
0.0090	2.91883	4.317577	5.791569
ε/D		Re = 10^6	
0.0000	4.565154	5.551406	6.299379
0.0011	4.144299	5.723025	7.367587
0.0045	3.900424	5.947677	8.202682
0.0090	3.809849	6.073447	8.702765
ε/D		Re = 5×10^6	
0.0000	12.77144	18.65604	22.11684
0.0011	6.417277	18.55552	28.59483
0.0045	5.987795	18.77076	33.07027
0.0090	6.306685	18.9334	**35.75453**

The coefficients of lift and drag have two contributing factors namely the pressure and shear stress differential across the body in the relevant direction. Lift is produced by a differential in pressure and shear stress between the suction and pressure sides of the cylinder, while drag is caused by a differential in pressure between the front and rear of the cylinder. The shear stress differential between the pressure and suction sides has a very small influence on the lift coefficient and contributes primarily to the drag coefficient. Therefore, lift is only dependent on the pressure differential between the suction and pressure surfaces. However, drag is influenced by both a pressure and shear stress differential. The corresponding components of drag are called the pressure and friction drag, respectively, while the overall drag is the sum total of these two components. The suction and pressure sides of the cylinder, as well as the front and the rear, are illustrated in Figure 8.
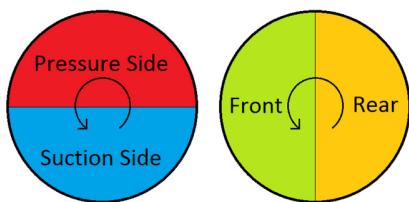

Figure 8: Cylinder convention

The lift force is proportional to the difference in pressure coefficient between the suction and pressure surfaces, plus the difference in skin friction between these surfaces. Similarly, the drag force is proportional to the difference in the pressure coefficient across the front and rear of the cylinder, plus the difference in skin friction coefficient across these surfaces. Therefore, the fundamental quantities that influence the lift and

drag coefficients are the pressure and skin friction coefficients. The influence of surface roughness, Reynolds number and non-dimensional rotation rate on these coefficients are summarised in Figures 8 and 9.

From Figure 8a it can be concluded that an increase in surface roughness leads to an increase in the negative suction side pressure coefficient between 0° and 150°. Between 180° and 270° a change in surface roughness shows little to no effect on the pressure coefficient. The pressure differential across the suction and pressure surfaces of the cylinder increases with increasing Reynolds number, which leads to an increasing lift, as illustrated in Figure 8b. From Figures 8c and 8d it follows that an increase in rotation rate leads to an increase in both the suction and pressure side pressure coefficients, therefore leading to an increase in the lift coefficient. Overall it can be concluded from Figure 8 that a rotating cylinder is indeed a lifting body since the negative suction side pressure coefficient is much greater in absolute magnitude than the positive pressure side pressure coefficient. Therefore, a pressure differential exists over the body and a resultant force known as lift is produced.

From Figure 9a it is evident that an increase in surface roughness leads to an increase in the average skin friction coefficient over the cylinder. Furthermore, from Figure 9b it follows that an increase in Reynolds number leads to a decrease in the average skin friction coefficient across the cylinder. It was found that the positive peaks in the friction coefficient graphs on the suction and pressure sides of the cylinder correspond to the separation points on the cylinder. The friction drag component decreases with an increase in Reynolds number, since the average skin friction coefficient decreases. This resulted in a decreasing drag coefficient with increasing Reynolds number. Furthermore, the separation points move towards one another with an increase in Reynolds number. This, combined with the decreasing skin friction coefficient leads to a decrease in both pressure and friction drag. The result is a decrease in the drag coefficient with an increase in Reynolds number. From Figures 9c and 9d it can be concluded that the average skin friction coefficient across the cylinder increases with increasing rotation rate. The separation points also move closer to one another leading to a decrease in the pressure drag, but an increase in the friction drag. The result is that at lower Reynolds numbers, the drag coefficient increases with an increase in rotation rate since the increase in friction drag is larger than the decrease in pressure drag. At larger Reynolds numbers it was found that an increase in rotation rate leads to a decrease in the drag coefficient since the decrease in pressure drag is now larger than the increase in friction drag.
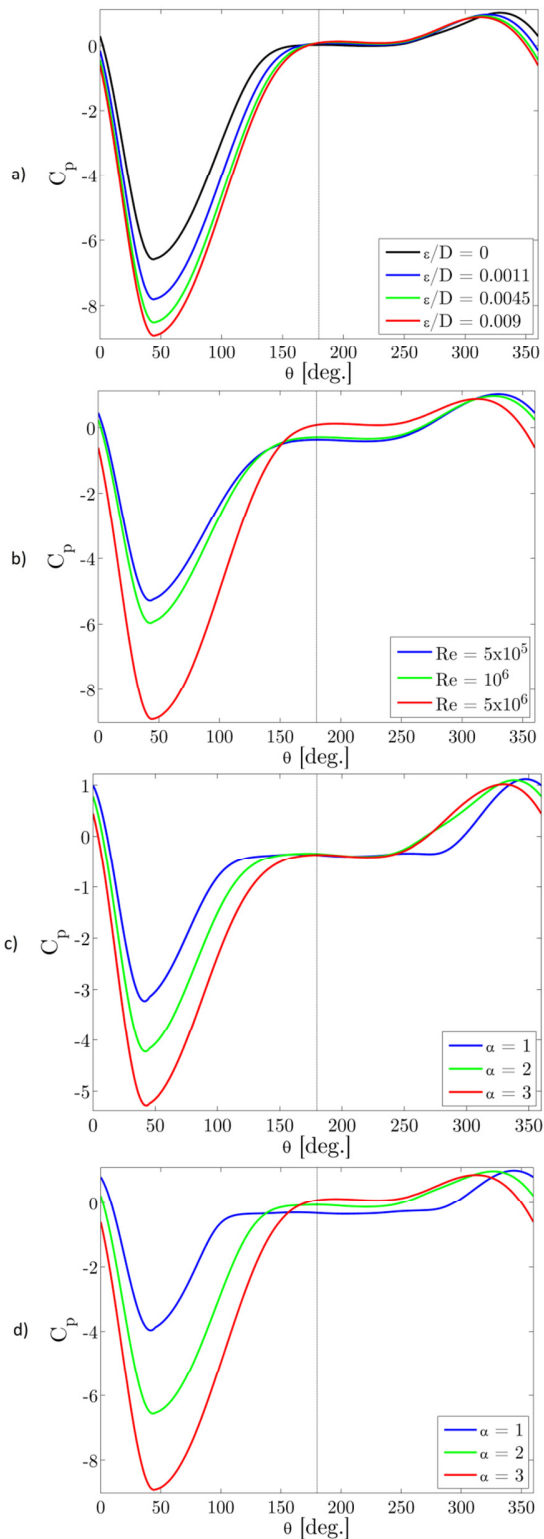
Figure 9: Pressure coefficient variation with a change in (a) surface roughness at Re = 5x10⁶ and α = 3, (b) Reynolds number at ε/D = 0.009 and α = 3, (c) non-dimensional rotation rate at Re = 5x10⁵ and ε/D = 0.009, (d) non-dimensional rotation rate at Re = 5x10⁶ and ε/D = 0.009.
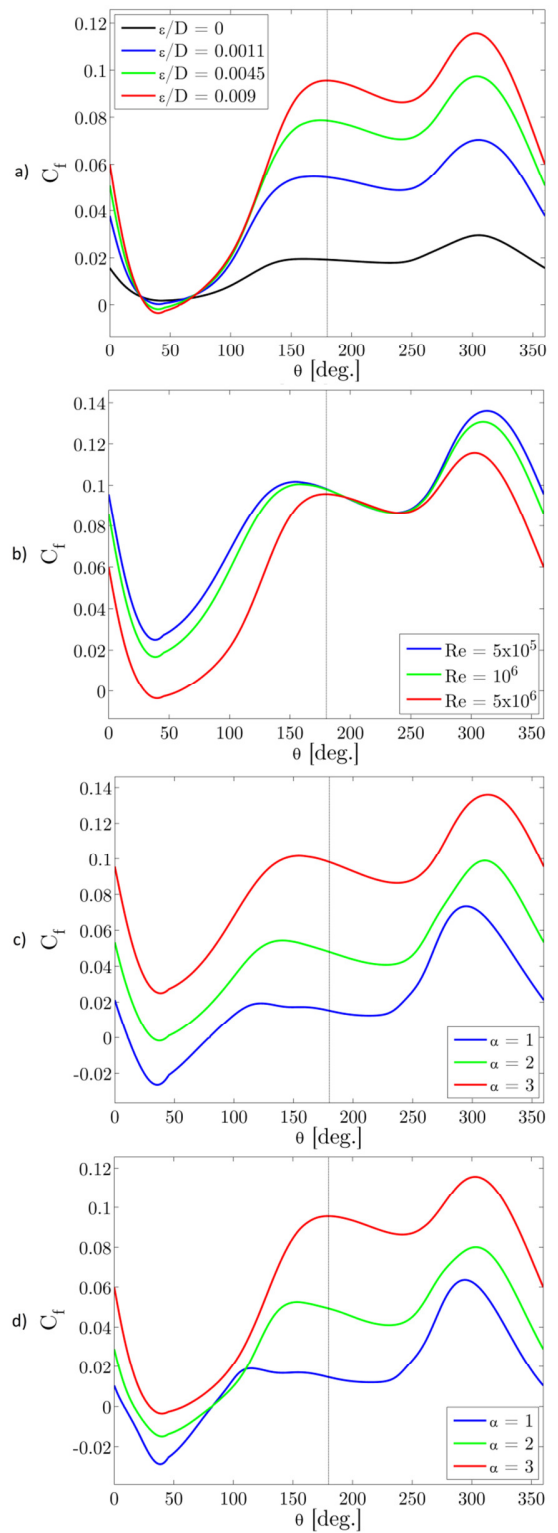
Figure 10: Skin friction coefficient variation with a change in (a) surface roughness at Re = 5x10⁶ and α = 3, (b) Reynolds number at ε/D = 0.009 and α = 3, (c) non-dimensional rotation rate at Re = 5x10⁵ and ε/D = 0.009, (d) non-dimensional rotation rate at Re = 5x10⁶ and ε/D = 0.009.

Although these figures only represent a fraction of the results, it is clear that the pressure and friction coefficients are influenced by a change in either surface roughness, Reynolds number or rotation rate. Increasing surface roughness or rotation rate leads to increasing pressure and friction. However, increasing Reynolds numbers leads to increasing pressure coefficients and decreasing friction coefficients.

The separation points for different combinations of Reynolds numbers, surface roughness and rotation rate are summarised in Tables 6 to 8. These separation points were obtained from the skin friction coefficient graphs. The positive peaks on the suction and pressure side of the cylinder correspond to the separation point on the suction and pressure side, respectively.

Table 6: Suction and pressure side separation points at $\alpha = 1$

		ε/D			
		0	0.0011	0.0045	0.009
Re = 5×10^5	Suction	122.7101	122.7101	122.7101	123.7448
	Pressure	285.0880	295.5926	297.2521	295.5926
Re = 10^6	Suction	123.7448	122.7101	122.7101	123.7448
	Pressure	283.7212	295.5926	297.2521	295.5926
Re = 5×10^6	Suction	120.6408	104.7006	108.6480	115.5558
	Pressure	279.6635	295.5926	296.4230	294.7635

Table 7: Suction and pressure side separation points at $\alpha = 2$

		ε/D			
		0	0.0011	0.0045	0.009
Re = 5×10^5	Suction	132.0221	132.0221	137.1954	141.3347
	Pressure	298.9102	311.1386	312.1257	311.1386
Re = 10^6	Suction	135.1260	135.1260	140.2997	144.4394
	Pressure	297.2521	311.1386	311.1386	310.1515
Re = 5×10^6	Suction	146.5093	145.4744	149.6141	154.7889
	Pressure	292.2763	306.3745	305.5441	303.8859

Table 8: Suction and pressure side separation points at $\alpha = 3$

		ε/D			
		0	0.0011	0.0045	0.009
Re = 5×10^5	Suction	141.3347	14.4394	150.6490	155.8238
	Pressure	315.0857	320.0199	316.0728	314.0986
Re = 10^6	Suction	144.4394	149.6141	155.8238	158.9286
	Pressure	313.1128	317.0599	313.1128	311.1386
Re = 5×10^6	Suction	160.9982	170.3078	175.4799	180.6523
	Pressure	306.3745	306.3745	304.7150	303.8859

From these tables it can be concluded that at low rotation rates the smooth cases exhibit smaller zones of separated flow when compared to the rough cases. On the other hand, at high rotation rates, the smooth cases have slightly larger zones of separated flow. For the rough cases it was found that an increase in surface roughness moves the separation points closer to one another, but although the size of the zone of separated flow reduces, the location of the separation bubble on the rear of the cylinder changes and thus leads to an increase in

drag coefficient with an increase in surface roughness. At lower rotation rates the separation points move further away from one another with an increase in Reynolds number while at higher rotation rates the separation points move closer to one another with an increase in Reynolds number. Finally, an increase in rotation rate leads to a decrease in the distance between the separation points.

CONCLUSION

This paper presented the CFD simulation results of turbulent flow across a rotating cylinder with surface roughness. From the results it was concluded that an increase in either surface roughness, Reynolds number or rotation rate led to an increase in both suction and pressure side pressure coefficients. This led to an increase in the pressure differential across the suction and pressure surfaces of the cylinder resulting in an increase in the lift coefficient. The drag coefficient increased with increasing surface roughness and rotation rate, but decreased with increasing Reynolds number. The separation points moved closer to one another with increasing rotation rate as well as Reynolds number, which led to a decreased pressure drag. Since the pressure drag component is more dominant at high Reynolds numbers, an increasing rotation rate led to a decreasing drag coefficient. The Reynolds number range investigated was found to be very desirable since the drag coefficient decreased and the lift coefficient increased with increasing Reynolds number. The aerodynamic efficiency increased with both Reynolds number and surface roughness at higher rotation rates, while an increase in the rotation rate also showed an overall increase in aerodynamic efficiency. The most aerodynamic efficient case occurred at a combination of the largest surface roughness, Reynolds number and rotation rate. However, this work is a part of an ongoing investigation regarding a wider range of rotation rates, surface roughness and Reynolds numbers.

ACKNOWLEDGEMENT

REFERENCES

[1] Stoijkovic, D., Breuer, M. & Durst, F., " Effect of high rotation rates on the laminar flow around a circular cylinder," *Physics of Fluids,* 14(9), 2002, pp. 3160-3178.

[2] Townsend, P., " A numerical simulation of newtonian and visco-elastic flow past stationary and rotating cylinders," *Journal of Non-Newtonian Fluid Mechanics,* Volume 6, 1979, pp. 219-243,.

[3] Badr, H. & Dennis, S., "Laminar forced convection from a rotating cylinder," *International Journal of Heat and Mass Transfer,* 28(1), 1985, pp. 253-264.

[4] Badr, H., Dennis, S. & Young, P., "Steady and unsteady flow past a rotating circular cylinder at low Reynolds numbers," *Computers & Fluids,* 17(4), 1989, pp. 579-609.

[5] Ingham, D. & Tang, T., "A numerical investigation into the steady flow past a rotating circular cylinder at low and

intermediate Reynolds numbers," *Journal of Computational Physics,* Volume 87, 1990, pp. 91-107.

[6] Tang, T. & Ingham, D., "On steady flow past a rotating circular cylinder at Reynolds numbers 60 and 100," *Computers & Fluids,* 19(2), 1991, pp. 217-230.

[7] Chiou, C. & Lee, S., "Forced convection on a rotating cylinder with an incident air jet,". *International Journal of Heat and Mass Transfer,* 36(15), 1993, pp. 3841-3850.

[8] Mittal, S. & Kumar, B., "Flow past a rotating cylinder," *Journal of Fuid Mechanics,* Volume 476, 2003, pp. 303-334.

[9] Lam, K., "Vortex shedding flow behind a slowly rotating circular cylinder," *Journal of Fluids and Structures,* Volume 25, 2009, pp. 245-262.

[10] Paramane, S. & Sharma, A., "Numerical investigation of heat and fluid across a rotating circular cylinder maintained as constant temperature in 2-D laminar flow regime," *International Journal of Heat and Mass Transfer,* Volume 52, 2009, pp. 3205-3216.

[11] Paramane, S. & Sharma, A., "Heat and fluid flow across a rotating cylinder dissipating uniform heat flux in 2D laminar flow regime," *International Journal of Heat and Mass Transfer,* Volume 53, 2010, pp. 4672-4683.

[12] Panda, S. & Chhabra, R., "Laminar flow of power-law fluids past a rotating cylinder," *Journal of Non-Newtonian Fluid Mechanics,* Volume 165, pp. 1442-1461, (2010).

[13] Elmiligui, A., Abdol-Hamid, K., Massey, S. & Pao, S., *Numerical study of flow past a circular cylinder using RANS, Hybrid RANS/LES and PANS formulations.* Rhode Island, American Institute of Aeronautics and Astronautics, 2004.

[14] Karabelas, S., "Large Eddy simulation of high-Reynolds number flow past a rotating cylinder," *International Journal of Heat and Fluid Flow,* Volume 31, 2010, pp. 518-527.

[15] Karabelas, S., Koumroglou, B., Argyropoulos, C. & Markatos, N., "High Reynolds number turbulent flow past a rotating cylinder". *Applied Mathematical Modelling,* Volume 36, 2012, pp. 379-398.

[16] Achenbach, E., "The effect of surface roughness on the heat transfer from a circular cylinder to the cross flow of air," *International Journal of Heat and Mass Transfer,* Volume 20, 1976, pp. 359-369.

[17] Dierich, F. & Nikrityuk, P., "A numerical study of the impact of surface roughness on heat and fluid flow past a cylindrical particle," *International Journal of Thermal Sciences,* Volume 65, 2013, pp. 92-103.

[18] Anderson, J., *Fundamentals of Aerodynamics,* New York: McGraw-Hill, (2011).

[19] Warschauer, K.A. & Leene, J.A.., Experiments on mean and fluctuating pressures of circular cylinders at cross flow at very high Reynolds numbers, *Proceedings of the International Conference on Wind Effects on Buildings and Structures*, Tokyo, 1971, pp.305-315.